Hydrothermal-assisted microwave extraction of bioactive phenolics and saponins from Curculigo orchioides

Chi Hai Tran
Ho Chi Minh City University of Industry and Trade
Thanh Sang Nguyen
Sai Gon Technology University
Van Man Phan
pvman.dbv@moet.edu.vn
Ba Ria–Vung Tau College of Technology

Research Article

Keywords: C. orchioides, polyphenols, ultrasonic-assisted extraction (MAE), response surface methodology, Global Natural Products Social Molecular Networking (GNPS)

Posted Date: June 3rd, 2026

DOI: https://doi.org/10.21203/rs.3.rs-9349976/v1

Additional Declarations: No competing interests reported.

Abstract

The rhizomes of *Curculigo orchioides* contain diverse phytochemicals associated with antioxidant and antidiabetic activities; however, efficient extraction of these compounds remains a challenge. In this study, hydrothermal pretreatment was applied prior to microwave-assisted extraction (MAE) to improve the release of intracellular metabolites from plant tissues. The extraction parameters, including solvent-to-solid ratio, microwave power, and extraction time, were optimized using response surface methodology based on a Box–Behnken experimental design with total phenolic content (TPC) and total saponin content (TSC) as response variables. The optimized MAE conditions were identified at approximately 40 mL/g, 300 W, and 30 min, resulting in TPC and TSC values of 73.15 mg GAE g^{-1} and 55.61 mg AE g^{-1}, respectively. Extracts obtained under these conditions showed strong radical-scavenging activity in DPPH and ABTS assays together with considerable α-glucosidase inhibitory activity. Microscopic observations indicated that pretreatment combined with microwave irradiation markedly disrupted the plant cellular matrix, which may facilitate the release of bioactive constituents. Comprehensive metabolite profiling using LC–MS/MS followed by GNPS-based molecular networking allowed the tentative annotation of 44 metabolites, including phenolic acids, phenolic glycosides, fatty acid derivatives, amino acid-related compounds, and several curculigoside-type metabolites commonly reported in *C. orchioides*. These results provide insight into the phytochemical composition of the extract and demonstrate the effectiveness of pretreatment-assisted MAE for recovering bioactive compounds from this medicinal plant.

1. Introduction

Medicinal plants are widely recognized as valuable sources of bioactive compounds with diverse pharmacological properties and potential applications in pharmaceuticals, nutraceuticals, and functional foods. Plant-derived secondary metabolites such as phenolics, flavonoids, terpenoids, and saponins have attracted considerable attention due to their antioxidant, anti-inflammatory, and metabolic regulatory activities, which may contribute to the prevention and management of chronic diseases including diabetes and cardiovascular disorders (El-Saadony et al., 2025; Mena & Angelino, 2020; Y. Wang et al., 2021). Consequently, medicinal plants continue to be extensively investigated as promising natural resources for bioactive compounds and functional ingredients.

Curculigo orchioides Gaertn., commonly known as black musli, is a medicinal herb belonging to the family Hypoxidaceae and widely distributed in tropical and subtropical regions of Asia, including India, China, Nepal, Vietnam, Laos, Malaysia, and the Philippines (Hejazi et al., 2018; Nie et al., 2013; Y. Wang et al., 2021). The plant typically grows in forest margins, grassy hillsides, and humid habitats with moderate shade and fertile soils, ranging from lowland areas to mountainous regions at elevations of up to approximately 2300 m (Nie et al., 2013; Y. Wang et al., 2021). Botanically, *C. orchioides* is a perennial herb characterized by a short underground rhizome with fleshy roots, narrow lanceolate leaves arranged in a basal rosette, and small yellow flowers emerging from the leaf axils. The rhizome represents the most important medicinal part and has long been used in traditional Chinese medicine and Ayurvedic

medicine as a tonic herb to enhance vitality and treat various disorders such as impotence, arthritis, asthma, jaundice, and metabolic diseases (Nie et al., 2013; Van Khiem et al., 2024; Y. Wang et al., 2021).

Extensive phytochemical investigations have revealed that *C. orchioides* contains a wide variety of secondary metabolites, including phenolic compounds, phenolic glycosides, triterpenoids, cycloartane-type saponins, flavonoids, lignans, alkaloids, and polysaccharides (Hejazi et al., 2018; Kushalan et al., 2022; Van Khiem et al., 2024). Among these constituents, phenolic glycosides and cycloartane-type saponins have been recognized as the principal bioactive compounds responsible for many of the pharmacological properties of the plant (Huong et al., 2025; Kushalan et al., 2022; Van Khiem et al., 2024). In particular, curculigoside and its derivatives are considered characteristic marker compounds of *C. orchioides* and have been reported to exhibit multiple biological activities, including antioxidant, anti-inflammatory, neuroprotective, anti-osteoporotic, immunomodulatory, and antidiabetic effects (Huong et al., 2025; Kushalan et al., 2022; Nie et al., 2013; Y. Wang et al., 2021). In addition to these compounds, other metabolites such as fatty acid derivatives, amino acid-related compounds, and various phenolic constituents have also been detected in the rhizomes, contributing to the overall biological activity of the plant extracts.

Phenolic compounds are known to play an important role in the antioxidant capacity of medicinal plants because of their ability to donate hydrogen atoms or electrons to neutralize reactive oxygen species and other free radicals (Mena & Angelino, 2020; Nie et al., 2013). As a result, extracts rich in phenolic constituents often exhibit strong radical-scavenging activity and inhibitory effects on enzymes involved in metabolic disorders (Mena & Angelino, 2020; Villegas-Aguilar et al., 2024). Several studies have reported that extracts of *C. orchioides* possess significant antioxidant, antidiabetic, and anti-inflammatory activities, which are attributed not only to phenolic glycosides such as curculigoside and orcinol derivatives but also to other bioactive metabolites including saponins and triterpenoids present in the rhizomes (Nie et al., 2013; Y. Wang et al., 2021).

Despite the well-documented medicinal value of *C. orchioides*, efficient extraction of its bioactive compounds remains a critical step for further phytochemical and pharmacological studies. Conventional extraction techniques often require long extraction times, large volumes of organic solvents, and may result in degradation of thermolabile compounds (Cao et al., 2025). In recent years, microwave-assisted extraction (MAE) has emerged as an effective green extraction technique capable of improving extraction efficiency, reducing solvent consumption, and shortening extraction time through rapid heating and enhanced cell disruption (Melikoglu, 2025; Singh et al., 2025). However, the extraction efficiency of MAE is strongly influenced by several operational parameters, including extraction temperature, microwave power, and extraction time. Therefore, systematic optimization of these parameters using statistical tools such as response surface methodology (RSM) is necessary to achieve optimal extraction conditions.

In addition to extraction efficiency, comprehensive characterization of the chemical composition of plant extracts is essential for understanding their biological activities. Although numerous studies have

focused on the isolation of individual compounds from *C. orchioides*, large-scale metabolite profiling of its extracts remains relatively limited. Recent advances in liquid chromatography–tandem mass spectrometry (LC–MS/MS) combined with molecular networking analysis have provided powerful metabolomics approaches for rapid annotation of metabolites in complex plant matrices. In particular, the Global Natural Products Social Molecular Networking (GNPS) platform enables visualization of structural relationships among metabolites based on MS/MS spectral similarity, facilitating the identification of compound families and the discovery of previously unreported metabolites (Huo et al., 2023; Jiang et al., 2025).

Therefore, the present study aimed to optimize microwave-assisted extraction conditions for the recovery of bioactive compounds from *Curculigo orchioides* rhizomes using response surface methodology. Furthermore, LC–MS/MS-based metabolite profiling combined with GNPS molecular networking analysis was employed to characterize the chemical composition of the extracts and to identify potential metabolites associated with their antioxidant properties.

2. Materials and Methods

2.1. Plant material and chemicals

Rhizomes of *Curculigo orchioides* Gaertn. were harvested at 16 months of cultivation from Quang Ngai Province, Vietnam. The rhizomes were washed thoroughly with distilled water, sliced into 2–3 mm sections, and dried in a forced-air oven at 55°C until constant weight (final moisture content 5–7%). The dried material was ground using a laboratory mill and sieved through a 1-mm mesh to obtain uniform particle size. The powdered samples were stored in airtight containers at 4°C protected from light until further use.

Absolute ethanol (≥ 99.5%), methanol (HPLC grade), acetonitrile (LC-MS grade), and formic acid (≥ 98%) were obtained from Merck (Darmstadt, Germany). Folin–Ciocalteu reagent, sodium carbonate (Na_2CO_3, ≥ 99%), vanillin (≥ 99%), sulfuric acid (95–98%), DPPH, ABTS, potassium persulfate, TPTZ, ferric chloride hexahydrate, and Trolox were purchased from Sigma-Aldrich (St. Louis, MO, USA). Gallic acid (≥ 99%) and aescin (≥ 98%) were used as reference standards for calibration of total phenolic content (TPC) and total triterpenoid content (TC), respectively. Ultrapure water was produced using a Milli-Q system (Millipore, USA). All reagents were of analytical grade or higher purity and used without further purification.

2.2. Hydrothermal pre-treatment combined with microwave-assisted extraction

To evaluate the potential enhancement effect of hydrothermal pre-treatment on ultrasound-assisted extraction (UAE), a preliminary comparative experiment was conducted prior to screening and multivariate optimization. Hydrothermal pre-treatment was carried out using a shaking water bath (WNB series, Memmert GmbH, Germany). A 5 g powdered *C. orchioides* rhizome (40–60 mesh) was mixed with 70% (v/v) aqueous ethanol at a solid-to-solvent ratio of 1:30 (g/mL) in tightly capped glass flasks (Jiang

et al., 2025). The mixtures were subjected to hydrothermal treatment at three different temperatures (60, 70, and 80°C) for 10, 20, and 30 min under continuous shaking. The treatment time was recorded after the solvent reached the preset temperature to ensure accurate control of thermal exposure. Upon completion, the samples were immediately cooled to room temperature in an ice-water bath to prevent further thermal effects.

Following pre-treatment, the mixtures were directly subjected to microwave-assisted extraction (MAE) using a laboratory microwave extraction system (MOB7816, Blustone, Vietnam) operating in closed-vessel mode with temperature control. In order to allow a direct comparison of the pre-treatment effect, the microwave parameters were kept constant at a temperature of 45°C, extraction time of 15 min, and microwave power of 440 W while maintaining the same solvent -to-solid ratio (30:1 mL/g) and solvent composition (70% aqueous ethanol). The treatment time was recorded after reaching the preset temperature.

For comparison, a control group without pre-treatment was prepared under identical microwave extraction conditions. After extraction, all samples were filtered and centrifuged at 5000 rpm for 10 min, and the supernatants were concentrated under reduced pressure prior to determination of total phenolic content (TPC) and total saponin content (TSC). For comparative purposes, Soxhlet extraction was carried out using 70% ethanol for 6 h under reflux conditions.

2.3. Microwave-assisted extraction and optimization

Microwave-assisted extraction (MAE) was carried out using a laboratory-scale microwave system (MOB7816, Blustone, Vietnam) equipped with temperature and power control. For each experiment, the powdered sample was mixed with aqueous ethanol (70%, v/v) in sealed microwave vessels and subjected to microwave irradiation under controlled conditions. To systematically evaluate the effects of processing parameters on extraction efficiency, a two-stage experimental design was implemented.

In the first stage, single-factor experiments were conducted to preliminarily assess the influence of key variables, including solvent -to-solid ratio (20–60 mL/g), microwave power (110–550 W), and extraction time (5–25 min). Each factor was varied individually while keeping the other parameters constant at their intermediate levels. The extraction performance was evaluated based on total phenolic content (TPC) and total saponin content (TSC). This preliminary screening aimed to determine suitable experimental ranges for subsequent multivariate optimization.

In the second stage, response surface methodology (RSM) based on a three-factor, three-level Box–Behnken design (BBD) was employed to investigate the combined effects of the selected variables. The solid-to-solvent ratio (X_1), microwave power (X_2), and extraction time (X_3) were selected as independent variables, while ethanol concentration was fixed at its intermediate level to reduce model complexity. A total of 17 experimental runs were generated according to the experimental design.

$$Y = \beta_0 + \sum_{i-1}^{n} \beta_i X_i + \sum_{i=1}^{n} \beta_{ii} X_i^2 + \sum_{i=1}^{n} \sum_{j=i+1}^{n} \beta_{ij} X_i X_j$$

1

where Y represents the predicted response and Xi denotes independent variables. Model adequacy was evaluated using analysis of variance (ANOVA), coefficient of determination (R^2), adjusted R^2, predicted R^2, and lack-of-fit testing. The model was subsequently used to predict extraction conditions that maximize the selected responses.

2.3. Determination of total phenolics, total saponins, and antioxidant activity

Total phenolic content (TPC), total saponin content (TSC), and antioxidant activity were determined spectrophotometrically using validated colorimetric assays.

TPC was quantified according to the Folin–Ciocalteu method with slight modifications (H. T. Tran et al., 2025). Briefly, 0.5 mL of appropriately diluted extract was mixed with 2.5 mL of ten-fold diluted Folin–Ciocalteu reagent and allowed to react for 5 min at room temperature. Subsequently, 2.0 mL of 7.5% (w/v) sodium carbonate solution was added, and the mixture was incubated in the dark for 30 min. The absorbance was measured at 765 nm using a UV–Vis spectrophotometer (Shimadzu UV-1800). Gallic acid (0–125 mg GAE/L) was used to construct the calibration curve ($R^2 \geq 0.995$), and the results were expressed as mg gallic acid equivalents per gram of dry weight (mg GAE/g DW).

TSC was determined using the vanillin–sulfuric acid colorimetric method as previously described (Bui et al., 2024). In brief, 0.5 mL of extract was mixed with 0.5 mL of 8% (w/v) vanillin solution in methanol, followed by the addition of 5 mL of freshly prepared 72% (v/v) sulfuric acid. The mixture was vortexed and incubated at 70°C for 10 min to allow chromophore development, then rapidly cooled in an ice bath to terminate the reaction. Absorbance was recorded at 550 nm. Aescin (10–200 mg AE/L) was used as the standard ($R^2 \geq 0.995$), and the results were expressed as mg aescin equivalents per gram of dry weight (mg AE/g DW). The obtained values represent the relative content of vanillin-reactive saponins in the extract.

Antioxidant activity was evaluated using DPPH radical scavenging assay. Briefly, 0.1 mL of extract at different concentrations (40 to 200 µg/mL) was mixed with 3.9 mL of 0.1 mM DPPH solution in methanol. The mixture was incubated in the dark for 30 min at room temperature, and the absorbance was measured at 517 nm. The radical scavenging activity was calculated as:

$$\text{Inhibition (\%)} = [(A_0 - A_1) / A_0] \times 100 \quad (2)$$

where A_0 is the absorbance of the control and A1 is the absorbance of the sample. The IC_{50} value (µg/mL), defined as the concentration of extract required to scavenge 50% of DPPH radicals, was determined by plotting inhibition percentage against extract concentration using nonlinear regression.

For the ABTS assay, the ABTS radical cation (ABTS•+) was generated by reacting

7 mM ABTS with 2.45 mM potassium persulfate and allowing the mixture to stand

in the dark for 16 h at room temperature (C. H. Tran et al., 2023). The resulting solution was diluted

with ethanol to obtain an absorbance of 0.70 ± 0.02 at 734 nm. Then, 0.1 mL of extract at various concentrations was mixed with 3.9 mL of the ABTS•+ solution. After incubation for 6 min at room temperature, the absorbance was measured at 734 nm. The percentage inhibition was calculated similarly to the DPPH assay, and the IC_{50} value (μg/mL) was obtained from the concentration–inhibition curve.

2.4. α-glucosidase inhibitory assay

The α-glucosidase inhibitory activity was evaluated with minor modifications of a previously reported method (Choi et al., 2023). Briefly, 20 μL of α-glucosidase solution (0.2 U/mL) was mixed with 20 μL of sample solution at different concentrations and 40 μL of phosphate buffer (pH 6.8). The mixture was pre-incubated at 37°C for 10 min. Then, 20 μL of 5 mM p-nitrophenyl-α-D-glucopyranoside (pNPG) was added to initiate the reaction. After incubation at 37°C for 20 min, 100 μL of 1 M Na_2CO_3 was added to terminate the reaction. Absorbance was measured at 405 nm using a microplate spectrophotometer. Acarbose was used as a positive control, and the reaction mixture without sample served as a negative control. Inhibitory activity was calculated as percentage inhibition relative to the control.

2.5. LC–MS/MS profiling and GNPS-based metabolite annotation

The chemical profile of the extract was analyzed using liquid chromatography coupled with tandem mass spectrometry (LC–MS/MS). Analyses were performed on an ExionLC™ system (SCIEX, USA) coupled to an X500R QTOF mass spectrometer (SCIEX, USA) equipped with a Hypersil GOLD C18 column (150 × 2.1 mm, 3 μm). The mobile phases consisted of (A) water containing 0.1% formic acid and (B) acetonitrile containing 0.1% formic acid. The gradient program was set as follows: 0–1 min, 98% A/2% B; 1–20 min, linear gradient to 2% A/98% B; and 20–25 min held at 2% A/98% B, at a flow rate of 0.40 mL min^{-1}.

Mass spectra were acquired using electrospray ionization in negative ion mode. Full-scan spectra were recorded over the m/z range 100–2000, followed by MS/MS acquisition over m/z 50–2000 under optimized collision energy conditions.

Raw LC–MS/MS data were converted to mzML format using MSConvert (ProteoWizard) and processed in MZmine 4 for feature detection, peak alignment, and filtering using the ADAP workflow [13–14]. Additional processing steps included isotope detection, gap filling, and ion identity networking, considering common adducts ($[M–H]^-$, $[M + Cl]^-$, $[M + FA]^-$, $[M+Acetate]^-$, $[M + Br]^-$) and neutral losses.

Metabolite annotation was performed using the Global Natural Products Social Molecular Networking (GNPS) platform by comparing experimental MS/MS spectra with public spectral libraries, including MassBank of North America and MS-DIAL libraries. Candidate metabolites were assigned based on accurate mass, fragmentation patterns, and spectral similarity. Spectral matching required at least two MS/MS spectra, a minimum of four matched fragment ions, and a cosine similarity score ≥ 0.7. The processed datasets were exported in MGF and CSV formats for subsequent GNPS molecular networking analysis.

2.6. Scanning electron microscopy (SEM) analysis

To enhance sample conductivity, a sputter coater was used to apply a thin gold film to the dried samples. The coated samples were subsequently examined using a scanning electron microscope (SEM; KYKY – 32000) at an accelerating potential of 30 kV and a magnification of 1000.

2.7. Statistical analysis

Experimental data were analyzed using Design – Expert 8.0.6 (Stat-Ease Inc., MN, USA). ANOVA was applied to assess the significance of model terms and variable interactions. All experiments were carried out in triplicate. Results are presented as mean ± SD, and statistical significance was set at $p < 0.05$.

3. Results and Discussion

3.1. Effect of hydrothermal pre-treatment on extraction efficiency

The data presented in Table 1 demonstrate that hydrothermal pre-treatment significantly influenced the recovery of total phenolic content (TPC) and total saponin content (TSC) from *Curculigo orchioides* rhizome.

Table 1
Comparative effects of hydrothermal pretreatment, direct microwave extraction, and Soxhlet extraction on TPC and TSC of *Curculigo orchioides*

Pretreatment condition	Extraction method	TPC (mg GAE/g DW)	TSC (mg AE/g DW)
None	Soxhlet (6h)	47.82^{e}±1.21	39.15^{c}±1.17
None	MAE (direct)	48.84^{e}±1.46	39.32^{c}±1.28
60°C – 10 min	MAE	55.92^{d}±1.38	46.05^{b}±1.21
60°C – 20 min	MAE	58.88^{c}±1.49	48.26^{b}±1.30
60°C – 30 min	MAE	60.11^{c}±1.35	48.72^{b}±1.24
70°C – 10 min	MAE	59.15^{c}±1.58	47.03^{b}±1.34
70°C – 20 min	MAE	67.92^{a}±1.62	52.47^{a}±1.39
70°C – 30 min	MAE	65.34±1.44	49.18^{ab}±1.32
80°C – 10 min	MAE	58.75^{c}±1.31	46.94^{b}±1.23
80°C – 20 min	MAE	56.63^{d}±1.27	44.86^{c}±1.29
80°C – 30 min	MAE	55.94^{d}±1.49	42.71^{c}±1.41

Values are expressed as mean ± standard deviation (n = 3). Different superscript letters within the same column indicate significant differences ($p < 0.05$).

Soxhlet extraction yielded 47.82 mg GAE/g DW (TPC) and 39.15 mg AE/g DW (TSC). Under identical solvent composition and solid–liquid ratio, direct microwave-assisted extraction (MAE) resulted in only marginal increases, reaching 48.84 mg GAE/g DW and 39.32 mg AE/g DW, corresponding to improvements of 2.1% and 0.4%, respectively, compared with Soxhlet extraction. These findings indicate that microwave heating alone, without prior structural modification, was insufficient to markedly enhance mass transfer from the intact plant matrix (Lee et al., 2016).

In contrast, hydrothermal pre-treatment prior to MAE substantially improved extraction efficiency. At 60°C, both TPC and TSC increased progressively with pre-treatment time, reaching 60.11 mg GAE/g DW and 48.72 mg AE/g DW after 30 min, representing increases of 25.7% and 24.5%, respectively, relative to Soxhlet extraction. The highest yields were obtained at 70°C for 20 min, where TPC and TSC reached 67.92 mg GAE/g DW and 52.47 mg AE/g DW, corresponding to improvements of 42.0% and 34.0%, respectively. The observed enhancement can be explained by thermally induced modification of the cellulose–hemicellulose–lignin matrix (Melikoglu, 2025; Singh et al., 2025). Moderate hydrothermal exposure likely promoted cell wall swelling, partial disruption of intermolecular hydrogen bonding, and increased tissue porosity, thereby reducing internal diffusion resistance. Subsequent microwave

irradiation facilitated rapid volumetric heating and internal pressure generation within pre-softened tissues, accelerating cell rupture and mass transfer of intracellular phenolics and saponins (Gao et al., 2021). However, excessive pre-treatment severity (80°C or prolonged exposure) led to reduced yields, possibly due to thermal degradation or instability of thermolabile constituents.

Overall, hydrothermal pre-treatment at 70°C for 20 min provided the most effective enhancement of MAE efficiency and was identified as the optimal condition. This optimized pre-treatment was therefore selected and fixed for the subsequent experiments, ensuring a structurally favorable matrix for further investigation and optimization of microwave-assisted extraction parameters.

3.2. Single factor experimental analysis

Figure 1A illustrates the influence of the solvent-to-solid ratio on the recovery of total phenolic content (TPC) and total saponin content (TSC) from *C. orchioides*. As the solvent-to-solid ratio increased from 20 to 50 mL/g, TPC rose markedly from approximately 20.13 to 69.56 mg GAE/g DW, representing more than a threefold increase. Similarly, TSC increased from about 31.00 mg AE/g at 20 mL/g to a maximum of 54.54 mg AE/g at 40 mL/g, followed by a slight decline at higher solvent volumes.

The enhancement observed at moderate solvent-to-solid ratios can be attributed to improved mass transfer efficiency. Increasing solvent volume enhances the concentration gradient between plant matrix and solvent, promotes solvent penetration into cellular structures, and facilitates the dissolution and diffusion of target compounds. These effects collectively contribute to the increased recovery of bioactive constituents. Similar trends have been widely reported in microwave-assisted extraction systems, where the solvent-to-solid ratio plays a critical role in extraction efficiency (Gao et al., 2021; Melikoglu, 2025; Sahal et al., 2025; Singh et al., 2025).

However, when the solvent-to-solid ratio was further increased to 60 mL/g, both TPC and TSC decreased, reaching approximately 52.14 mg GAE/g and 33.20 mg AE/g, respectively. This decline may be attributed to the excessive solvent volume, which can dilute the concentration of extracted compounds and reduce microwave energy absorption efficiency, thereby limiting the effective interaction between microwave energy and the sample matrix. In addition, overly high solvent volumes may reduce the localized heating effect, leading to less efficient cell disruption and compound release. Based on these results, a solvent-to-solid ratio of 50 mL/g was selected as the optimal condition to achieve high recovery of both TPC and TSC.

Figure 1B presents the effect of microwave power on extraction efficiency, with temperature and extraction time fixed at 45°C and 25 min, respectively. TPC increased significantly from 31.14 mg GAE/g at 110 W to 71.80 mg GAE/g at 440 W, while TSC increased from 35.35 mg AE/g to a maximum of 54.13 mg AE/g at 330 W. The increase in extraction yield with increasing microwave power can be explained by enhanced volumetric heating and internal pressure generation within plant cells, which promote cell wall rupture and facilitate the release of intracellular compounds (Gao et al., 2021; Sahal et al., 2025). However, when the power was further increased to 550 W, both TPC and TSC declined to 67.45 mg

GAE/g and 45.24 mg AE/g, respectively. This decrease may be attributed to overheating and localized thermal degradation of bioactive compounds under excessive microwave energy input (Cavalluzzi et al., 2022; López-Salazar et al., 2023; Zhang et al., 2019). Therefore, 440 W was identified as the most suitable microwave power, providing the highest TPC and a relatively high TSC.

Figure 1C shows the influence of extraction time on compound recovery. Both TPC and TSC increased significantly from 5 to 15 min, with TPC rising from 23.10 to 71.10 mg GAE/g and TSC increasing from 33.40 to 54.34 mg AE/g. This initial increase reflects rapid mass transfer and efficient release of readily extractable compounds during the early stage of extraction. Beyond 15 min, a gradual decrease was observed, with TPC declining to 68.56 mg GAE/g at 20 min and 60.15 mg GAE/g at 25 min, and TSC decreasing accordingly. This decline may be associated with prolonged thermal exposure, leading to degradation, oxidation, or structural modification of bioactive compounds (Hoang et al., 2025; Zhang et al., 2019). Consequently, 15 min was selected as the optimal extraction time.

Based on the results of the single-factor experiments, a Box–Behnken design (BBD) was employed for further optimization. A total of 17 experimental runs were conducted to evaluate the combined effects of three independent variables: solid to solvent ratio (20–60 mL/g), microwave power (110–550 W), and extraction time (5–25 min). These ranges were selected based on the optimal intervals identified above. Response surface methodology (RSM) was subsequently applied to model the interactions among variables and to determine the optimal conditions for maximizing TPC and TSC extraction.

3.3. Response surface modelling and process interpretation

The influence of solvent-to-solid ratio (X_1), microwave power (X_2), and extraction time (X_3) on total phenolic content (TPC) and total saponin content (TSC) was systematically investigated using response surface methodology (RSM) based on a Box–Behnken design (Table 2). Both responses exhibited substantial variation within the studied domain, confirming that bioactive compound recovery from *Curculigo orchioides* is strongly governed by processing conditions and nonlinear interactions among variables.

Table 2
Box–Behnken experimental design and observed responses for total phenolic content (TPC) and total saponin content (TSC).

Run	X_1: Extraction temperature (℃)	X_2: Microwave power (W)	X_3: Extraction time (min)	TPC (mg GAE/g DW)	TSC (mg AE/g DW)
1	40	350	5	34.1	39.6
2	40	350	45	60.15	45.1
3	40	250	25	71.9	54.4
4	40	150	45	44.78	40.15
5	60	350	25	67.2	48.2
6	60	250	5	55.14	42.56
7	40	250	25	70.9	54
8	20	250	45	58.41	43.5
9	60	250	45	60.14	45.16
10	40	150	5	28.15	35.67
11	20	150	25	32.13	38.5
12	20	350	25	50.19	41.98
13	40	250	25	70	54
14	60	150	25	56.19	42.15
15	20	250	5	29.05	36.45

The developed quadratic models were highly significant for both responses, with F-values of 44.57 ($p = 0.0003$) for TPC and 271.02 ($p < 0.0001$) for TSC (Table 3). These results indicate that the selected independent variables collectively explain a statistically significant proportion of the experimental variability. The coefficients of determination were notably high ($R^2 = 0.988$ for TPC and $R^2 = 0.998$ for TSC), demonstrating excellent goodness-of-fit (Zhang et al., 2019).

Table 3
Regression analysis and model fitting statistics for TPC and TSC extraction models.

Source of variance (TPC)	**Sum of squares**	***df***	**Mean square**	**F value**	**P value**	**Significance**
X_1-Extraction temperature (°C)	593.229	1	593.229	69.881	0.0004	significant
X_2-Microwave power (W)	317.394	1	317.394	37.388	0.0017	
X_3-Extraction time (min)	741.895	1	741.895	87.393	0.0002	
$X_1 \times X_2$	12.426	1	12.426	1.464	0.281*	
$X_1 \times X_3$	148.352	1	148.352	17.4755	0.00865	
$X_2 \times X_3$	22.184	1	22.184	2.613	0.167*	
X_1^2	117.503	1	117.503	13.842	0.0137	
X_2^2	779.657	1	779.657	91.841	0.00021	
X_3^2	861.369	1	861.369	101.467	0.00017	
Residual	42.445	5	8.490			
Lack of Fit	38.106	3	12.702	5.853	0.149	not significant
Pure Error	4.340	2	2.170			
Cor Total	3447.950	14				
Std. Dev.	2.914		R^2	0.988		
Mean	52.695		Adjusted R^2	0.965		
C.V. %	5.529		Predicted R^2	0.821		
			Adeq Precision	19.019		
Source of variance (TSC)	**Sum of squares**	**df**	**Mean square**	**F value**	**P value**	**Significance**
Model	548.491	9	60.944	271.018	3.5E-06	significant
X_1-Extraction temperature (°C)	38.896	1	38.896	172.973	4.5E-05	

The p-value was used to evaluate the statistical significance of individual model coefficients as well as the interaction effects among independent variables. * indicates a statistically insignificant effect ($p > 0.05$).

Source of variance (TPC)	Sum of squares	*df*	Mean square	F value	P value	Significance
X_2-Microwave power (W)	42.366	1	42.366	188.404	3.7E-05	
X_3-Extraction time (min)	48.167	1	48.167	214.201	2.7E-05	
$X_1 \times X_2$	1.652	1	1.652	7.345	0.04229	
$X_1 \times X_3$	4.951	1	4.951	22.016	0.00538	
$X_2 \times X_3$	0.260	1	0.260	1.157	0.3310*	
X_1^2	91.786	1	91.786	408.174	5.5E-06	
X_2^2	169.396	1	169.396	753.311	1.2E-06	
X_3^2	211.215	1	211.215	939.282	6.9E-07	
Residual	1.125	5	0.225			
Lack of Fit	0.618	3	0.206	0.813	0.593	not significant
Pure Error	0.508	2	0.253			
Cor Total	549.616	14				
Std. Dev.	0.474		R^2	0.998		
Mean	44.161		Adjusted R^2	0.994		
C.V. %	1.074		Predicted R^2	0.980		
			Adeq Precision	48.651		

The p-value was used to evaluate the statistical significance of individual model coefficients as well as the interaction effects among independent variables. * indicates a statistically insignificant effect ($p > 0.05$).

A distinction was observed in predictive performance. For TSC, the close agreement between adjusted R^2 (0.994) and predicted R^2 (0.980) confirms strong model stability and high predictive reliability (Sahal et al., 2025; Zhang et al., 2019). In contrast, although the TPC model exhibited a high adjusted R^2, its predicted R^2 (0.8203) was comparatively lower, suggesting slightly reduced predictive robustness outside the experimental domain. This behavior implies that phenolic extraction may be more sensitive to variations in solvent-to-solid ratio and microwave conditions compared with saponins.

The lack-of-fit was not significant ($p > 0.05$) for either response, confirming that no systematic deviation exists between experimental and predicted values. Furthermore, the Adequate Precision ratios (19.02 for

TPC and 48.65 for TSC) were substantially higher than the minimum required value of 4, indicating excellent signal-to-noise discrimination and validating the suitability of the regression models for optimization and process design.

Model adequacy was further confirmed through residual diagnostics (Fig. 2). In the normal probability plots, the externally studentized residuals for both TPC and TSC closely followed the linear reference line, indicating that the residuals were normally distributed (Xue et al., 2021). The residuals versus predicted plots displayed random dispersion around zero without noticeable patterns, confirming homoscedasticity and independence of errors. No data points exceeded the critical ± 6.25 residual limits, indicating the absence of influential outliers. Notably, the residual distribution for TSC appeared more compact than that for TPC, which is consistent with its higher predictive R^2 and overall model stability.

$$Y_1 = 71.60 + 8.61X_1 + 6.30X_2 + 9.63X_3 - 4.99X_1^2 - 6.78X_2^2 - 7.56X_3^2 - 6.09X_1X_2 \quad (3)$$

$$Y_2 = 54.47 + 2.20X_1 + 2.30X_2 + 2.45X_3 - 4.82X_1^2 - 6.61X_2^2 - 7.40X_3^2 + 1.65X_1X_2 + 4.95X_2X_3 \quad (4)$$

For TPC, all three linear factors significantly influenced phenolic recovery ($p < 0.05$), demonstrating that increasing solvent-to-solid ratio, microwave power, and extraction time enhanced phenolic diffusion within the tested range. This enhancement can be attributed to improved solvent availability, enhanced concentration gradients, and microwave-induced cell disruption, which collectively facilitate mass transfer and solute release (Hoang et al., 2025; Xue et al., 2021; Zhang et al., 2019). In particular, the solvent-to-solid ratio plays a critical role in governing extraction efficiency by controlling the driving force for diffusion and solute solubility (Han et al., 2019; Su et al., 2022).

However, the highly significant negative quadratic terms (X_1^2, X_2^2, X_3^2), particularly those associated with microwave power and extraction time, revealed pronounced curvature in the response surface. These findings indicate that beyond moderate processing intensity, the benefits of increased solvent volume and energy input are offset by dilution effects and reduced microwave energy density, as excessive solvent can absorb and dissipate microwave energy less efficiently (J. Chen et al., 2020; Dall'Acqua et al., 2009). In addition, phenolic compounds are prone to oxidative degradation under prolonged microwave exposure (Lu, 2023).

Interestingly, among the interaction terms, only the combined effect of solvent-to-solid ratio and extraction time (X_1X_3) was statistically significant, suggesting that prolonged extraction at high solvent volumes may reduce extraction efficiency due to weakened localized heating and lower effective energy transfer (J. Chen et al., 2020). In contrast, simultaneous increases in solvent-to-solid ratio and microwave power did not produce a significant synergistic effect. This statistical behavior was visually supported by dome-shaped 3D surfaces and elliptical contour plots (Fig. 3A–C), where TPC reached its maximum at moderate solvent-to-solid ratios (approximately 40–50 mL/g), intermediate microwave power (250–330 W), and controlled extraction time (25–30 min), but declined under excessive solvent volumes (60 mL/g) combined with high energy input.

Although TSC was also significantly affected by all three linear factors ($p < 0.001$), its response pattern exhibited greater statistical stability and smoother curvature compared to TPC. Microwave power exerted the strongest linear contribution, followed by extraction time and solvent-to-solid ratio, confirming that energy input is the primary driver for saponin release through effective matrix disruption (Hoang et al., 2025; Xue et al., 2021). Unlike TPC, TSC displayed two significant interaction terms (X_1X_2 and X_1X_3), indicating that solvent-to-solid ratio interacts synergistically with both microwave power and extraction time in influencing saponin extraction.

Nevertheless, the highly significant negative quadratic coefficients for X_1^2, X_2^2, and X_3^2 confirm that excessive solvent volume or prolonged processing reduces TSC, likely due to dilution effects and possible structural destabilization of saponin molecules under extended microwave exposure (Dall'Acqua et al., 2009; Lu, 2023). The smoother and more symmetrical 3D response surfaces observed for TSC are consistent with its lower experimental variability (C.V. = 1.07%) and stronger predictive reliability (Fig. 3D–F).

A comparative analysis of both responses highlights a fundamental difference in sensitivity to processing conditions. TPC appears more sensitive to variations in solvent-to-solid ratio and microwave intensity, whereas TSC demonstrates greater stability under similar conditions. This difference has been widely attributed to the higher susceptibility of phenolic compounds to oxidation and environmental stress compared with saponins, which generally exhibit greater structural robustness (Lu, 2023; Z.-H. Wang et al., 2013).

3.4. Optimization of shaking pretreatment–MAE and integrated bioactivity interpretation

The extraction conditions were optimized using response surface methodology (RSM), which predicted optimal parameters at 40.24 mL/g, 289.66 W, and 29.88 min. For practical implementation, these values were adjusted to 40 mL/g, 300 W, and 30 min. Under these conditions, the shaking pretreatment–MAE process yielded total phenolic content (TPC) and total saponin content (TSC) values of 73.15 mg GAE/g d.m. and 55.61 mg AE/g d.m., respectively. The experimental values were in close agreement with the predicted values within the 95% confidence interval, confirming the reliability of the developed RSM model.

Significant differences in phytochemical recovery were observed among the extraction methods (Table 4, $p < 0.05$). The MAE process combined with shaking pretreatment produced the highest TPC (72.92 mg GAE/g DW) and TSC (55.47 mg AE/g DW), which were substantially higher than those obtained using Soxhlet extraction (47.82 and 39.15 mg/g DW, respectively) and direct MAE (48.84 and 39.32 mg/g DW). This represents an increase of approximately 50% in phenolic recovery compared with conventional Soxhlet extraction. The enhanced extraction efficiency can be attributed to the shaking pretreatment step, which improves solvent penetration and matrix hydration prior to microwave irradiation, thereby facilitating rapid cell disruption and more efficient release of intracellular phytochemicals.

Table 4
Antioxidant activity and α-glucosidase inhibitory activity of *C. orchioides* extracts obtained by different extraction methods

Extraction method	TPC (mg GAE/g DW)	TSC (mg AE/g DW)	DPPH (IC50: µg/mL)	ABTS (IC50: µg /mL)	α-Glucosidase inhibition (µg /mL)
MAE + shaking	72.92^{a}±1.62	55.47^{a}±1.39	68.76^{a}±1.58	56.67^{a}±1.42	140.11^{b}±1.27
Soxhlet	47.82^{b}±1.21	39.15^{b}±1.17	80.63^{b}±1.44	65.64^{b}±1.36	176.13^{c}±1.33
MAE (direct)	48.84^{b}±1.46	39.32^{b}±1.28	82.05 ± 1.51	68.21 ± 1.29	166.16 ± 1.22
Acarbose (control)			–	–	29.30^{a} ± 0.88

Values are expressed as mean ± standard deviation (n = 3). Different superscript letters within the same column indicate significant differences ($p < 0.05$).

The improved phytochemical recovery was reflected in the biological activities of the extracts. The optimized extract exhibited the strongest antioxidant capacity, as indicated by the lowest IC_{50} values in both DPPH (68.76 µg/mL) and ABTS (56.67 µg/mL) assays. In comparison, Soxhlet extraction showed moderate activity (80.63 and 65.64 µg/mL, respectively), whereas direct MAE displayed the weakest radical scavenging ability (82.05 and 68.21 µg/mL). The stronger antioxidant activity of the optimized extract is consistent with its higher phenolic content, since phenolic compounds can effectively donate hydrogen atoms or electrons to stabilize free radicals (López-Salazar et al., 2023; Sahal et al., 2025; Zhang et al., 2019).

A similar trend was observed for α-glucosidase inhibitory activity. The shaking pretreatment–MAE extract exhibited the strongest inhibition among the plant extracts, with an IC_{50} value of 140.11 µg/mL, followed by direct MAE (166.16 µg/mL) and Soxhlet extraction (176.13 µg/mL). Although the inhibitory activity was weaker than that of the pharmaceutical inhibitor acarbose (IC_{50} = 29.30 µg/mL), the extract still demonstrated considerable enzyme inhibitory potential. This activity may be associated with the presence of phenolic compounds and triterpenoid saponins in *Curculigo orchioides*, which have been reported to interact with the catalytic site of α-glucosidase and inhibit carbohydrate hydrolysis (Han et al., 2019; Su et al., 2022).

Structural observations obtained from scanning electron microscopy (Fig. 4) further supported these findings. The untreated plant material displayed intact and compact cellular structures with smooth surfaces. Soxhlet-treated samples showed moderate swelling and limited cell disruption, indicating relatively slow solvent diffusion during prolonged heating. In contrast, MAE-treated samples exhibited pronounced structural damage. Particularly, the shaking pretreatment–MAE sample showed extensive cell wall rupture and porous structures, which significantly increased the surface area and facilitated the release of intracellular phytochemicals.

3.5. GNPS-Based molecular networking analysis and metabolite annotation

To further elucidate the chemical constituents responsible for the observed bioactivities, the LC–MS/MS dataset obtained from the optimized extract was analyzed using the Global Natural Products Social Molecular Networking (GNPS) platform. Molecular networking enables the visualization of structurally related metabolites based on MS/MS spectral similarity, thereby facilitating the annotation of compounds sharing common fragmentation patterns (Fig. 5). Using this approach, a total of 44 metabolites were tentatively annotated based on accurate mass measurements, adduct ion formation, retention time, and comparison with spectral libraries and literature data (Table 5).

Table 5
LC–MS/MS-based tentative identification of metabolites in *Curculigo orchioides* via GNPS molecular networking

Identified metabolite	**Mass ion**	**R_t**	***m/z***	**Mass**	**Error (ppm)**
Tilarginine	[M + H]+	1.13	189.1336	189.1346	5.3
Carnitine	[M + H]+	1.18	162.1116	162.1125	5.36
D-(+)-Cellobiose	[M + H-H2O]+	1.24	325.1118	325.1129	3.45
Sucrose	[M + H]+	1.24	343.1225	343.1235	2.88
Melibiose	[M + Na]+	1.24	365.1032	365.1054	6.11
Lauryldiethanolamine	[M + H]+	11.77	274.2716	274.2741	8.95
12-hydroxy-stearic-acid	[M+NH4]+	11.89	318.2989	318.3003	4.3
6-hydroxy-hexanoic-acid_1-decanol	[M+NH4]+	11.96	290.2677	290.269	4.37
(6Z,9Z,12Z)-octadeca-6,9,12-trienoic-acid	[M + H]+	17.69	279.2306	279.2319	4.5
Arginyl-lysyl-methionine	[M + H-2H2O]+	17.7	398.2308	398.2333	6.2
1-Hexadecanoyl-sn-glycerol	[M + H]+	18.63	331.2826	331.2843	5.09
9-Octadecenamide, (Z)-	[M + H]+	18.81	282.2778	282.2791	4.75
3-hydroxyl-5-methyphenol-1-O-[β-D-glucopyranosyl-(1->3)-β-D-glucopyranoside]	[M+NH4]+	5.39	466.1898	466.1919	4.5
Orcinol glucoside	[M + H]+	5.43	287.1114	287.1125	3.93
Melezitose	[M + Na]+	1.24	527.1569	527.1583	2.57
Adenosine	[M + H]+	4.34	268.1033	268.104	2.72
Lauramidopropyl betaine	[M]+	12.36	343.294	343.2955	4.43
Galaxolidone	[M + H]+	15.87	273.1838	273.1849	4.05
Chlorogenic acid	[M + H]+	6.11	355.1011	355.1024	3.54
Syringic acid	[M + H]+	5.34	199.0595	199.0601	3.01
Sakakin	[M + H]+	5.39	287.1111	287.1125	4.98
1',3'-dimethoxyl-4-hydroxyalangifolioside	[M + Na]+	8.33	489.1339	489.1367	5.78

Identified metabolite	Mass ion	R_t	*m/z*	Mass	Error (ppm)
12α,16β-dihydroxy-3β-[(O-α-L-rhamnopyranosyl-(1->2)-β-D-glucopyranosyl)oxy]-9,19-cyclolanostan-24-one	[M + Na]+	11.13	805.4659	805.4709	6.16
Orcinoside F	[M + Na]+	5.75	441.1343	441.1367	5.51
Orcinoside D	[M + H]+	5.8	257.1011	257.102	3.36
2-6-dimethoxybenzoic acid	[M + H]+	8.33	183.0646	183.0652	3.19
2-hydroxy-6-methoxybenzoic acid; 6-methoxysalicylic acid; 6-methoxysalicyclic acid	[M + H]+	5.15	169.0487	169.0495	4.94
4-ethoxy-3-hydroxymethylphenol	[M + Na]+	5.39	191.0694	191.0679	8.05
4-hydroxy-benzoic acid	[M + H-H2O]+	15.94	121.0279	121.0284	4.17
4-methylheptadecanoic acid	[M+NH4]+	13.09	302.3033	302.3054	6.79
Chlorocurculigoside C	[M + Na]+	8.21	583.0927	583.0956	4.91
Chlorocurculigoside D	[M+NH4]+	8.11	548.128	548.1296	2.93
Curculigine B	[M + Na]+	8.66	523.0722	523.0744	4.27
Curculigoside B	[M + Na]+	7.93	475.1191	475.1211	4.17
Curculigoside C	[M + Na]+	7.16	505.1298	505.1316	3.65
Glucosyringic acid	[M + Na]+	5.34	383.0932	383.0949	4.35
Orcinol	[M + H]+	5.39	125.0591	125.0597	4.84
2,4,6-Trimethylpyridine	[M + H]+	4.78	122.0957	122.0964	5.94
Tryptophan	[M + H]+	5.66	205.0964	205.0972	3.67
Lauryldimethylamine Oxide	[M + H]+	11.84	230.2473	230.2478	2.35
Phytosphingosine	[M + H]+	13.12	318.2987	318.3003	4.93
2,6-Dimethoxybenzoic acid	[M + H]+	8.28	183.0642	183.0652	5.38
Curculigoside	[M + Na]+	8.3	489.1338	489.1367	5.99
Heriguard	[M + Na]+	6.15	377.0827	377.0843	4.24

The generated molecular network revealed several clusters corresponding to structurally related metabolite classes, including phenolic acids, phenolic glycosides, carbohydrates, amino acid derivatives,

lipid-related compounds, and triterpenoid glycosides. Such clustering reflects the structural relationships among metabolites and has been widely applied for rapid chemical profiling of complex plant extracts.

Among the detected metabolites, phenolic acids represented an important group of antioxidant constituents. For example, chlorogenic acid was detected at *m/z* 355.1011 ($[M + H]^+$), while syringic acid appeared at *m/z* 199.0595 ($[M + H]^+$) (Table 5 and Fig. 6). Additional phenolic derivatives including 2,6-dimethoxybenzoic acid (*m/z* 183.0642 $[M + H]^+$), 2-hydroxy-6-methoxybenzoic acid (*m/z* 169.0487 $[M + H]^+$), and 4-hydroxybenzoic acid (*m/z* 121.0279 $[M + H–H_2O]^+$) were also detected in the network. Phenolic acids are widely distributed in medicinal plants and are well known for their radical-scavenging properties, primarily attributed to hydroxylated aromatic rings capable of donating hydrogen atoms or electrons to neutralize reactive oxygen species [24, 30].

A prominent cluster (I) in the molecular network corresponded to orcinol-type phenolic glycosides, which are recognized as characteristic secondary metabolites of *Curculigo orchioides* (Fig. 6). In this cluster, orcinol glucoside (*m/z* 287.1114 $[M + H]^+$), orcinoside D (*m/z* 257.1011 $[M + H]^+$), and orcinoside F (*m/z* 441.1343 $[M + Na]^+$) were annotated. In addition, the glycosylated phenolic compound 3-hydroxy-5-methylphenol-1-O-[β-D-glucopyranosyl-(1→3)-β-D-glucopyranoside] was detected at *m/z* 466.1898 ($[M + NH_4]^+$). Orcinol-derived phenolic glycosides have frequently been reported in phytochemical studies of *C. orchioides* and are considered chemotaxonomic markers of this species, contributing to its diverse pharmacological activities.

In addition to orcinol derivatives, several curculigoside-type phenolic glycosides were identified, which are regarded as major bioactive constituents of *C. orchioides*. These included curculigoside (*m/z* 489.1338 $[M + Na]^+$), curculigoside B (*m/z* 475.1191 $[M + Na]^+$), curculigoside C (*m/z* 505.1298 $[M + Na]^+$), and curculigine B (*m/z* 523.0722 $[M + Na]^+$) [31]. Furthermore, chlorinated derivatives such as chlorocurculigoside C (*m/z* 583.0927 $[M + Na]^+$) and chlorocurculigoside D (*m/z* 548.1280 $[M + NH_4]^+$) were also tentatively annotated. Previous studies have demonstrated that curculigoside-type phenolic glycosides possess various biological activities, including antioxidant, anti-inflammatory, neuroprotective, and antidiabetic effects, highlighting their importance as key bioactive compounds in *C. orchioides* (X. Chen et al., 2017; Z.-H. Wang et al., 2013).

Besides phenolic metabolites, the molecular network also revealed the presence of a triterpenoid glycoside. Specifically, 12α,16β-dihydroxy-3β-[(O-α-L-rhamnopyranosyl-(1→2)-β-D-glucopyranosyl)oxy]-9,19-cyclolanostan-24-one was tentatively annotated at *m/z* 805.4659 ($[M + Na]^+$, *t*R = 11.13 min) (Table 5). This compound belongs to the cycloartane-type triterpenoid glycosides, characterized by a 9,19-cyclolanostane skeleton linked to a disaccharide moiety composed of rhamnose and glucose (Yokosuka et al., 2010). The MS/MS spectrum displayed characteristic fragment ions around *m/z* 779 and 468, which are consistent with the sequential loss of sugar units and partial cleavage of the triterpenoid backbone. Cycloartane-type triterpenoids have been widely reported in medicinal plants and are known to exhibit diverse pharmacological activities, including antioxidant, anti-inflammatory, and immunomodulatory effects (Hu et al., 2021). The detection of this compound

therefore indicates that, besides phenolic metabolites, terpenoid glycosides may also contribute to the biological activity of the extract.

In addition to specialized secondary metabolites, several primary metabolites were also detected. Carbohydrates such as sucrose (*m/z* 343.1225 $[M + H]^+$), D-(+)-cellobiose (*m/z* 325.1118 $[M + H–H_2O]^+$), melibiose (*m/z* 365.1032 $[M + Na]^+$), and melezitose (*m/z* 527.1569 $[M + Na]^+$) were observed at early retention times. Amino acid-related compounds including tilarginine (*m/z* 189.1336 $[M + H]^+$), carnitine (*m/z* 162.1116 $[M + H]^+$), tryptophan (*m/z* 205.0964 $[M + H]^+$), and arginyl-lysyl-methionine (*m/z* 398.2308 $[M + H–2H_2O]^+$) were also identified. Additionally, several lipid-related metabolites were detected, such as 12-hydroxystearic acid (*m/z* 318.2989 $[M + NH_4]^+$), (6Z,9Z,12Z)-octadeca-6,9,12-trienoic acid (*m/z* 279.2306 $[M + H]^+$), phytosphingosine (*m/z* 318.2987 $[M + H]^+$), and 9-octadecenamide (*m/z* 282.2778 $[M + H]^+$).

The predominance of phenolic acids and phenolic glycosides in the optimized extract provides a plausible explanation for the strong antioxidant activity observed in the DPPH and ABTS assays. Phenolic compounds such as chlorogenic acid and syringic acid possess well-established radical-scavenging properties due to their ability to donate electrons or hydrogen atoms to neutralize free radicals (Srinivasulu et al., 2018; Yokosuka et al., 2010). Moreover, curculigoside-type glycosides isolated from *Curculigo orchioides* have previously been reported to exhibit significant antioxidant and enzyme inhibitory activities (Hou et al., 2025). Therefore, the abundance of these metabolites likely contributed to the relatively low IC_{50} values obtained in the antioxidant assays.

Overall, the GNPS-based molecular networking analysis revealed a chemically diverse metabolite profile dominated by phenolic acids and curculigoside-type phenolic glycosides, accompanied by triterpenoid glycosides and several primary metabolites. These findings provide a comprehensive overview of the metabolite composition of the optimized extract and offer a plausible chemical basis for its observed antioxidant potential.

4. Conclusion

This study demonstrates that the integration of hydrothermal pretreatment with microwave-assisted extraction (MAE) improves the recovery of bioactive constituents from the rhizomes of Curculigo orchioides. Pretreatment at 70°C for 20 min effectively modified the plant tissue structure, facilitating mass transfer and promoting the release of intracellular metabolites during microwave extraction. Response surface methodology identified solvent-to-solid ratio, microwave power, and extraction time as key factors affecting phytochemical recovery. Under the optimized conditions (approximately 40 mL/g, 300 W, and 30 min), the extract contained relatively high levels of total phenolics (73.15 mg GAE g^{-1}) and total saponins (55.61 mg AE g^{-1}). These phytochemical enrichments were consistent with the stronger antioxidant capacity observed in DPPH and ABTS assays as well as the pronounced α-glucosidase inhibitory activity. Microscopic observation further indicated that the combined pretreatment–MAE process induced substantial disruption of plant cell structures, which likely facilitated the release of

intracellular compounds. LC–MS/MS analysis coupled with GNPS-based molecular networking enabled the tentative annotation of 44 metabolites, including phenolic acids, phenolic glycosides, fatty acid derivatives, amino acid derivatives, and several curculigoside-related compounds characteristic of *C. orchioides*. The occurrence of these metabolites provides a chemical basis for the biological activities observed in the extracts. The results highlight the effectiveness of combining pretreatment, optimized MAE, and LC–MS/MS metabolite profiling for improving the extraction and characterization of bioactive compounds from *C. orchioides*. This approach may support the further utilization of this medicinal plant as a natural source of antioxidant and enzyme-inhibitory compounds for functional food and nutraceutical applications.

Declarations

Conflict of Interest:

The authors have no relevant financial or non-financial interests to disclose.

Funding:

No funding was received for conducting this study.

Author Contribution

Chi Hai Tran : Conceptualization, Investigation, Methodology, Data curation, Validation, Formal analysis, Software, Writing- original draft. Thanh Sang Nguyen : Data curation, Validation, Formal analysis, Software. Van Man Phan : Conceptualization, Investigation, Methodology, Data curation, Software, Formal analysis, Writing- review & editing.

Acknowledgments:

The authors gratefully acknowledge the support and research facilities provided by Ho Chi Minh City University of Industry and Trade, Sai Gon Technology University, and Ba Ria – Vung Tau College of Technology, Vietnam.

Data Availability

The authors have confirmed that the data supporting this study can be found in the article

References

1. Bui TD, Do LTK, Dang TND, Pham VD, Hoang VC (2024) Recovery of Saponins, Phenolic Compounds and Antioxidant Capacity from Curculigo orchioides Gaertn Rhizomes by Different Extraction Methods. Appl Sci 14(17):7535. https://doi.org/10.3390/app14177535
2. Cao S, Liang J, Chen M, Xu C, Wang X, Qiu L, Zhao X, Hu W (2025) Comparative analysis of extraction technologies for plant extracts and absolutes. In *Frontiers in Chemistry*. Front Media SA 13. https://doi.org/10.3389/fchem.2025.1536590
3. Cavalluzzi MM, Lamonaca A, Rotondo NP, Miniero DV, Muraglia M, Gabriele P, Corbo F, De Palma A, Budriesi R, De Angelis E, Monaci L, Lentini G (2022) Microwave-Assisted Extraction of Bioactive Compounds from Lentil Wastes: Antioxidant Activity Evaluation and Metabolomic Characterization. Molecules 27(21). https://doi.org/10.3390/molecules27217471
4. Chen J, Yang J, Ma L, Li J, Shahzad N, Kim CK (2020) Structure-antioxidant activity relationship of methoxy, phenolic hydroxyl, and carboxylic acid groups of phenolic acids. Sci Rep 10(1). https://doi.org/10.1038/s41598-020-59451-z
5. Chen X, Zuo A, Deng Z, Huang X, Zhang X, Geng C, Li T, Chen J (2017) New phenolic glycosides from Curculigo orchioides and their xanthine oxidase inhibitory activities. Fitoterapia 122:144–149. https://doi.org/10.1016/j.fitote.2017.09.009
6. Choi GY, Han YS, Sim KH, Kim MH (2023) Phenolic compounds, antioxidant capacity, and α-amylase and α-glucosidase inhibitory activity of ethanol extracts of perilla seed meal. Food Sci Nutr 11(8):4596–4606. https://doi.org/10.1002/fsn3.3419
7. Dall'Acqua S, Shrestha BB, Comai S, Innocenti G, Gewali MB, Jha PK (2009) Two phenolic glycosides from Curculigo orchioides Gaertn. Fitoterapia 80(5):279–282. https://doi.org/10.1016/j.fitote.2009.03.002
8. El-Saadony MT, Saad AM, Mohammed DM, Alkafaas SS, Abd El-Mageed TA, Fahmy MA, Ahmed E, Algopishi A, Abu-Elsaoud UB, Mosa AM, AbuQamar WFA, S. F., El-Tarabily KA (2025) Plant bioactive compounds: extraction, biological activities, immunological, nutritional aspects, food application, and human health benefits—A comprehensive review. In *Frontiers in Nutrition*. Front Media SA 12. https://doi.org/10.3389/fnut.2025.1659743
9. Gao Y, Remón J, Matharu AS (2021) Microwave-assisted hydrothermal treatments for biomass valorisation: a critical review. In *Green Chemistry* (Vol. 23, Number 10, pp. 3502–3525). Royal Society of Chemistry. https://doi.org/10.1039/d1gc00623a
10. Han Y, Chi J, Zhang M, Zhang R, Fan S, Huang F, Xue K, Liu L (2019) Characterization of saponins and phenolic compounds: Antioxidant activity and inhibitory effects on α-glucosidase in different varieties of colored quinoa (Chenopodium quinoa Willd). Bioscience Biotechnol Biochem 83(11):2128–2139. https://doi.org/10.1080/09168451.2019.1638756
11. Hejazi II, Khanam R, Mehdi SH, Bhat AR, Rizvi MMA, Thakur SC, Athar F (2018) Antioxidative and anti-proliferative potential of Curculigo orchioides Gaertn in oxidative stress induced cytotoxicity: In vitro, ex vivo and in silico studies. Food Chem Toxicol 115:244–259. https://doi.org/10.1016/j.fct.2018.03.013

12. Hoang TNN, Luu TQH, Nguyen A, V., Le THA (2025) Optimization of extraction and structural characterization of bioactive compounds from Musa balbisiana peel. Sci Rep 15(1). https://doi.org/10.1038/s41598-025-24874-z
13. Hou Y, Liang C, Sui L, Li Y, Wang K, Li X, Zheng K, Su H, Xie D, Lin D, Guo D, Wang L (2025) Curculigoside Regulates Apoptosis and Oxidative Stress Against Spinal Cord Injury by Modulating the Nrf-2/NQO-1 Signaling Pathway In Vitro and In Vivo. Mol Neurobiol 62(3):3082–3097. https://doi.org/10.1007/s12035-024-04409-9
14. Hu M, Zhao D, Xu X, Ma G, Wu H, Chen X (2021) Actaticas A – G, Cycloartane Triterpenes From Actaea asiatica With Their Antiproliferative Activity. *Frontiers in Chemistry*, *9*. https://doi.org/10.3389/fchem.2021.695456
15. Huo C, Nguyen QN, Alishir A, Ra MJ, Jung SM, Yu JN, Gwon HJ, Kang KS, Kim KH (2023) Global Natural Products Social (GNPS)-Based Molecular-Networking-Guided Isolation of Phenolic Compounds from Ginkgo biloba Fruits and the Identification of Estrogenic Phenolic Glycosides. Plants 12(23). https://doi.org/10.3390/plants12233970
16. Huong LT, Bach VD, Hai PT, Thao VM, Nhiem NX, Dang NH (2025) Cycloartane-type saponins from Curculigo orchioides and their anti-inflammatory activity. RSC Adv 15(49):41340–41350. https://doi.org/10.1039/d5ra04849d
17. Jiang H, Dong Y, Pan S, Zhou H, Cui H (2025) Optimization of the Extraction Process and Comprehensive Evaluation of the Antimicrobial and Antioxidant Properties of Different Polar Parts of the Ethanol Extracts of Cannabis sativa L. ACS Omega 10(17):17453–17467. https://doi.org/10.1021/acsomega.4c10986
18. Kushalan S, Yathisha UG, Khyahrii S, A., Hegde S (2022) Phytochemical and anti-oxidant evaluation of in vitro and in vivo propagated plants of Curculigo orchioides. Vitro Cell Dev Biology - Plant 58(3):382–391. https://doi.org/10.1007/s11627-021-10246-5
19. Lee CS, Binner E, Winkworth-Smith C, John R, Gomes R, Robinson J (2016) Enhancing natural product extraction and mass transfer using selective microwave heating. Chem Eng Sci 149:97–103. https://doi.org/10.1016/j.ces.2016.04.031
20. López-Salazar H, Camacho-Díaz BH, Ocampo A, M. L., Jiménez-Aparicio AR (2023) Microwave-assisted Extraction of Functional Compounds from Plants: A Review. BioResources 18(3):6614–6638. https://doi.org/10.15376/biores.18.3.Lopez-Salazar
21. Lu X (2023) Changes in the structure of polysaccharides under different extraction methods. In *eFood* (Vol. 4, Number 2). John Wiley and Sons Inc. https://doi.org/10.1002/efd2.82
22. Melikoglu M (2025) Microwave-assisted extraction: Recent advances in optimization, synergistic approaches, and applications for green chemistry. In *Sustainable Chemistry for Climate Action* (Vol. 7). Elsevier B.V. https://doi.org/10.1016/j.scca.2025.100122
23. Mena P, Angelino D (2020) Plant food, nutrition, and human health. In *Nutrients* (Vol. 12, Number 7, pp. 1–5). MDPI AG. https://doi.org/10.3390/nu12072157

24. Nie Y, Dong X, He Y, Yuan T, Han T, Rahman K, Qin L, Zhang Q (2013) Medicinal plants of genus Curculigo: Traditional uses and a phytochemical and ethnopharmacological review. In *Journal of Ethnopharmacology* (Vol. 147, Number 3, pp. 547–563). https://doi.org/10.1016/j.jep.2013.03.066
25. Sahal A, Hussain A, Mishra R, Pandey S, Dobhal A, Ahmad W, Kumar V, Lohani UC, Kumar S (2025) Microwave-assisted extraction of bioactive compounds from Urtica dioica using solvent-based process optimization and characterization. Sci Rep 15(1). https://doi.org/10.1038/s41598-025-09855-6
26. Singh T, Shafı Z, Singh R, Bisht B, Yadav KK, Algethami JS, Albakri GS, Alreshidi MA (2025) Microwave-assisted extraction of phytochemicals from Piper betle L.: Optimization, characterization, and bioactivity evaluation. Food Chemistry: X 29. https://doi.org/10.1016/j.fochx.2025.102672
27. Srinivasulu C, Ramgopal M, Ramanjaneyulu G, Anuradha CM, Suresh Kumar C (2018) Syringic acid (SA) – A Review of Its Occurrence, Biosynthesis, Pharmacological and Industrial Importance. In *Biomedicine and Pharmacotherapy* (Vol. 108, pp. 547–557). Elsevier Masson SAS. https://doi.org/10.1016/j.biopha.2018.09.069
28. Su R, Li J, Hu N, Wang H, Cao J, Chi X, Dong Q (2022) Screening for α-Glucosidase-Inhibiting Saponins from Pressurized Hot Water Extracts of Quinoa Husks. Foods 11(19). https://doi.org/10.3390/foods11193026
29. Tran CH, Nghiem MT, Dinh AMT, Dang TTN, Van Do TT, Chu TN, Mai TH, Phan VM (2023) Optimization Conditions of Ultrasound-Assisted Extraction for Phenolic Compounds and Antioxidant Activity from Rubus alceifolius Poir Leaves. *International Journal of Food Science*, *2023*. https://doi.org/10.1155/2023/7576179
30. Tran HT, Tran TTA, Ly CG, Tran TH, Tran TT, Tran TKN (2025) Optimization of the Extraction of Antioxidant Components from Curculigo orchioides Gaertn Rhizomes by Ultrasound-Assisted Enzymatic Extraction. J Oleo Sci 74(8):709–720. https://doi.org/10.5650/jos.ess25042
31. Van Khiem N, Duc M, N., Thanh Giang D (2024) *Bioactive Compounds and Biological Activities of Curculigo orchioides Gaertn*. https://doi.org/10.5772/intechopen.1007137
32. Villegas-Aguilar MdelC, Sánchez-Marzo N, Fernández-Ochoa Á, Río D, Montaner C, Micol J, Herranz-López V, Barrajón-Catalán M, Arráez-Román E, de la Cádiz-Gurrea D L., Segura-Carretero A (2024) Evaluation of Bioactive Effects of Five Plant Extracts with Different Phenolic Compositions against Different Therapeutic Targets. Antioxidants 13(2). https://doi.org/10.3390/antiox13020217
33. Wang Y, Li J, Li N (2021) Phytochemistry and Pharmacological Activity of Plants of Genus Curculigo: An Updated Review Since 2013. Molecules 26(11):3396. https://doi.org/10.3390/molecules26113396
34. Wang Z-H, Huang J, Ma X-C, Li G-Y, Ma Y-P, Li N, Wang J-H (2013) Phenolic glycosides from Curculigo orchioides Gaertn. Fitoterapia 86:64–69. https://doi.org/10.1016/j.fitote.2013.01.008
35. Xue H, Tan J, Fan L, Li Q, Cai X (2021) Optimization microwave-assisted extraction of anthocyanins from cranberry using response surface methodology coupled with genetic algorithm and kinetics

model analysis. J Food Process Eng 44(6). https://doi.org/10.1111/jfpe.13688

36. Yokosuka A, Sato K, Mimaki Y (2010) Cycloartane glycosides from the rhizomes of Curculigo orchioides. Phytochemistry 71(17–18):2174–2181. https://doi.org/10.1016/j.phytochem.2010.09.005
37. Zhang H, Birch J, Ma ZF, Xie C, Yang H, Bekhit AED, Dias G (2019) Optimization of microwave-assisted extraction of bioactive compounds from New Zealand and Chinese Asparagus officinalis L. roots. J Food Sci Technol 56(2):799–810. https://doi.org/10.1007/s13197-018-3540-0

Figures

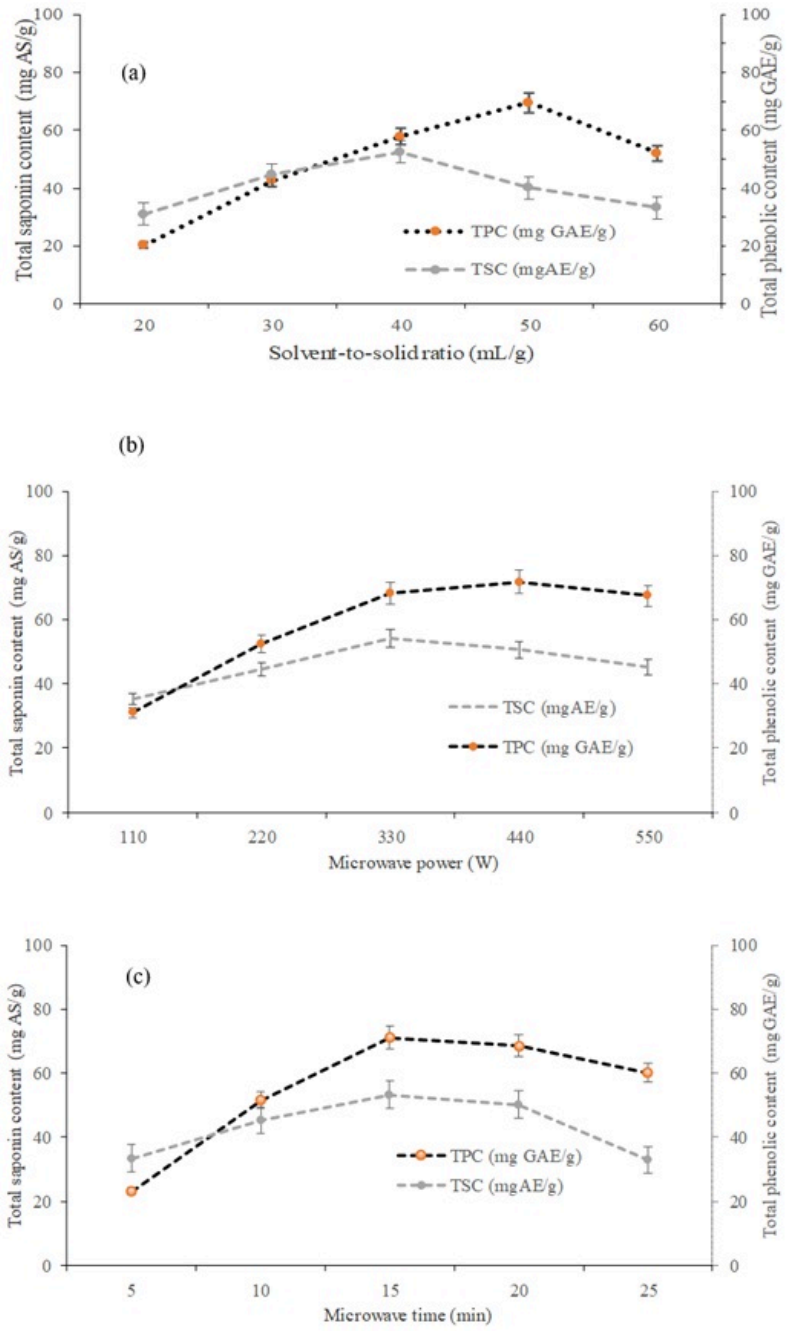

Figure 1

Effect of (a) solvent to solid ratio; (b) microwave power and (c) extraction time on TPC and TSC

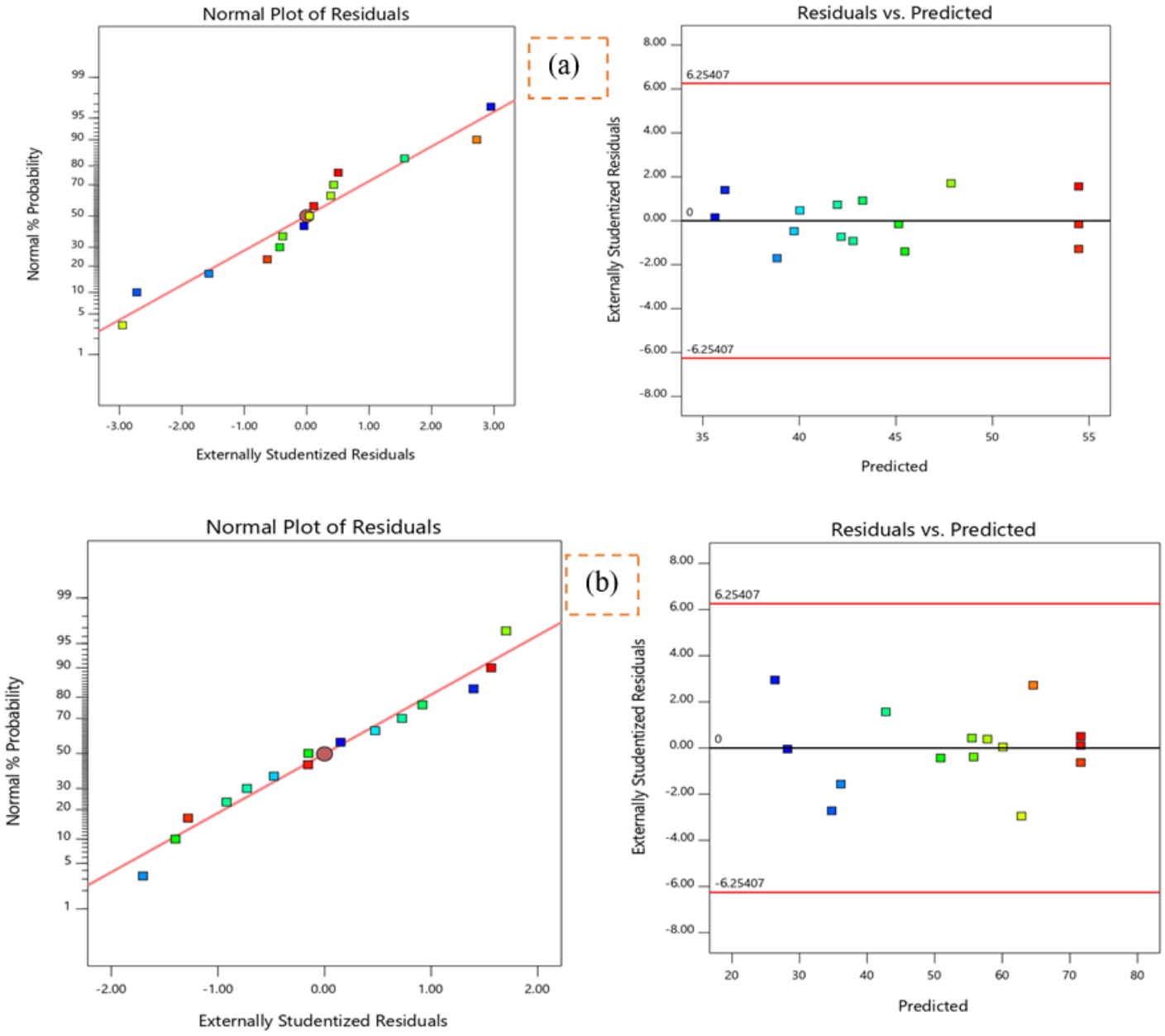

Figure 2

Diagnostic plots for model adequacy of (a) total phenolic content (TPC) and (b) total saponin content (TSC): normal probability plots of externally studentized residuals and residuals versus predicted values.

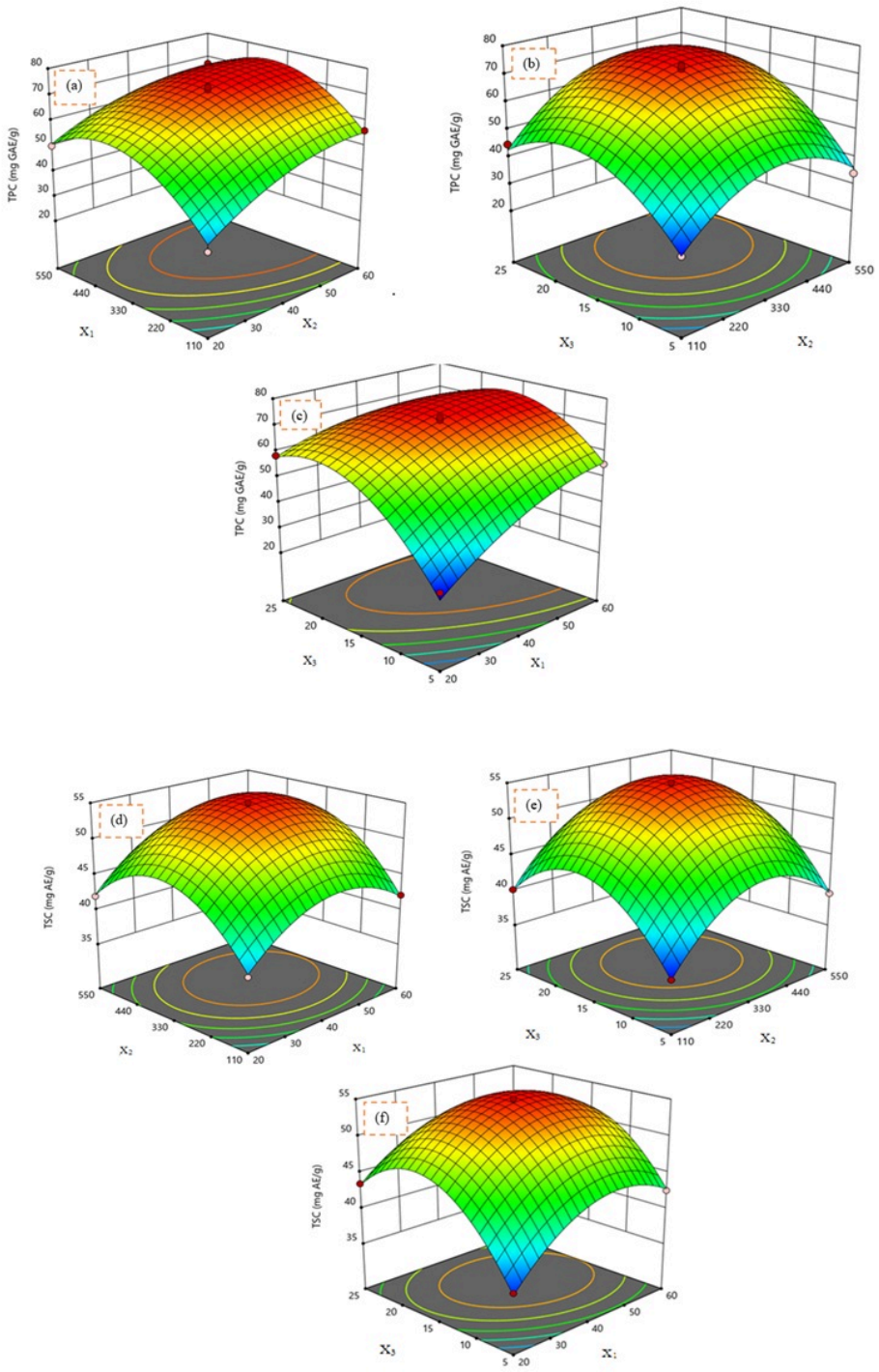

Figure 3

Response surface and contour plots showing the effects solvent to solid ratio (X_1, mL/g), microwave power (X_2, W), and extraction time (X_3, min) on TPC (A–C) and TSC (D–F) of *C. orchioides*.

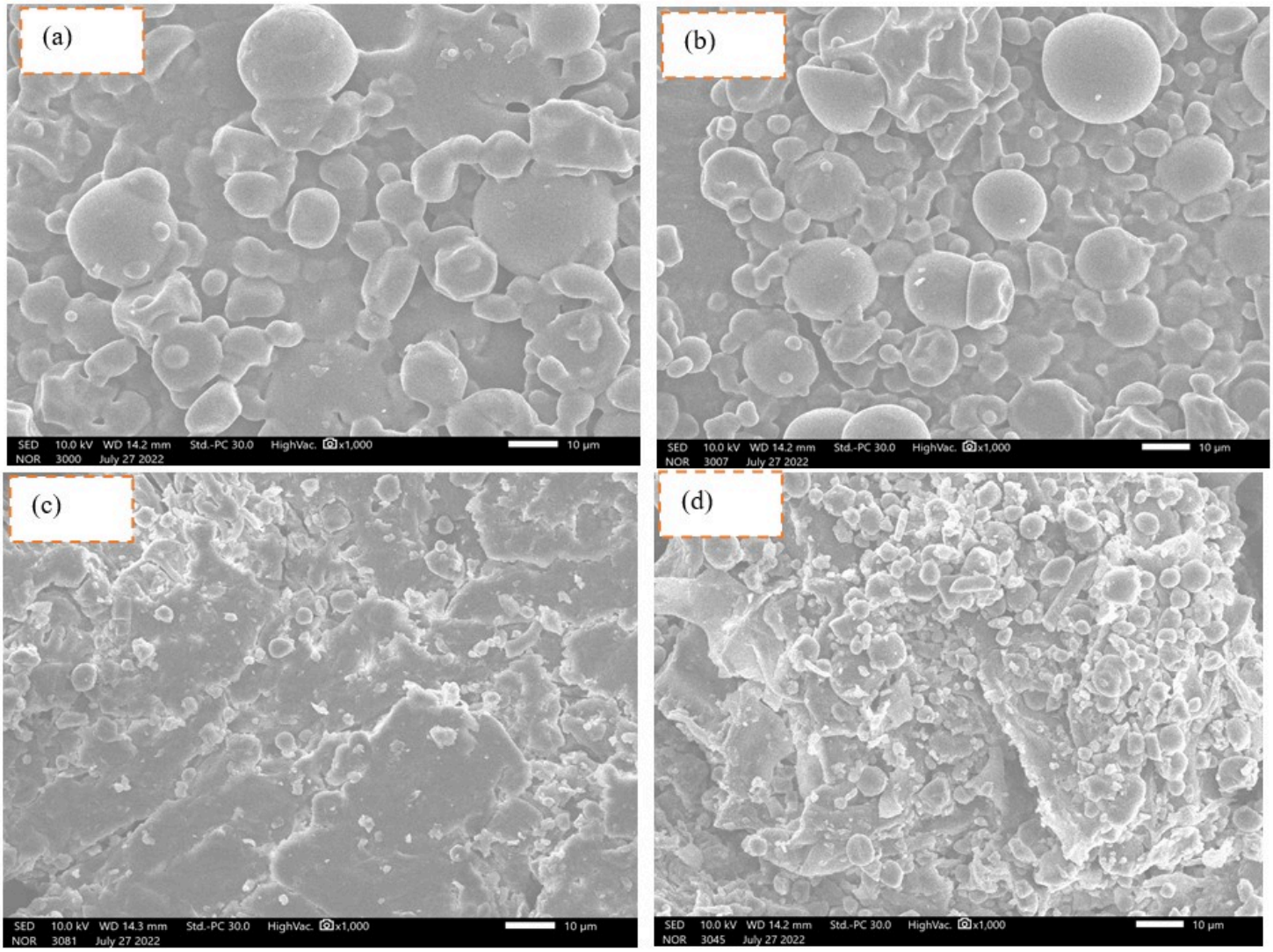

Figure 4

SEM micrographs of C. *orchioides* before and after extraction using different techniques: (a) raw material, (b) conventional soxhlet extraction, (c) MAE without shaking at optimal condition, (d) Shaking pretreatment–MAE process, showing progressive cell wall disruption at 1,000× mag

(A)

nification

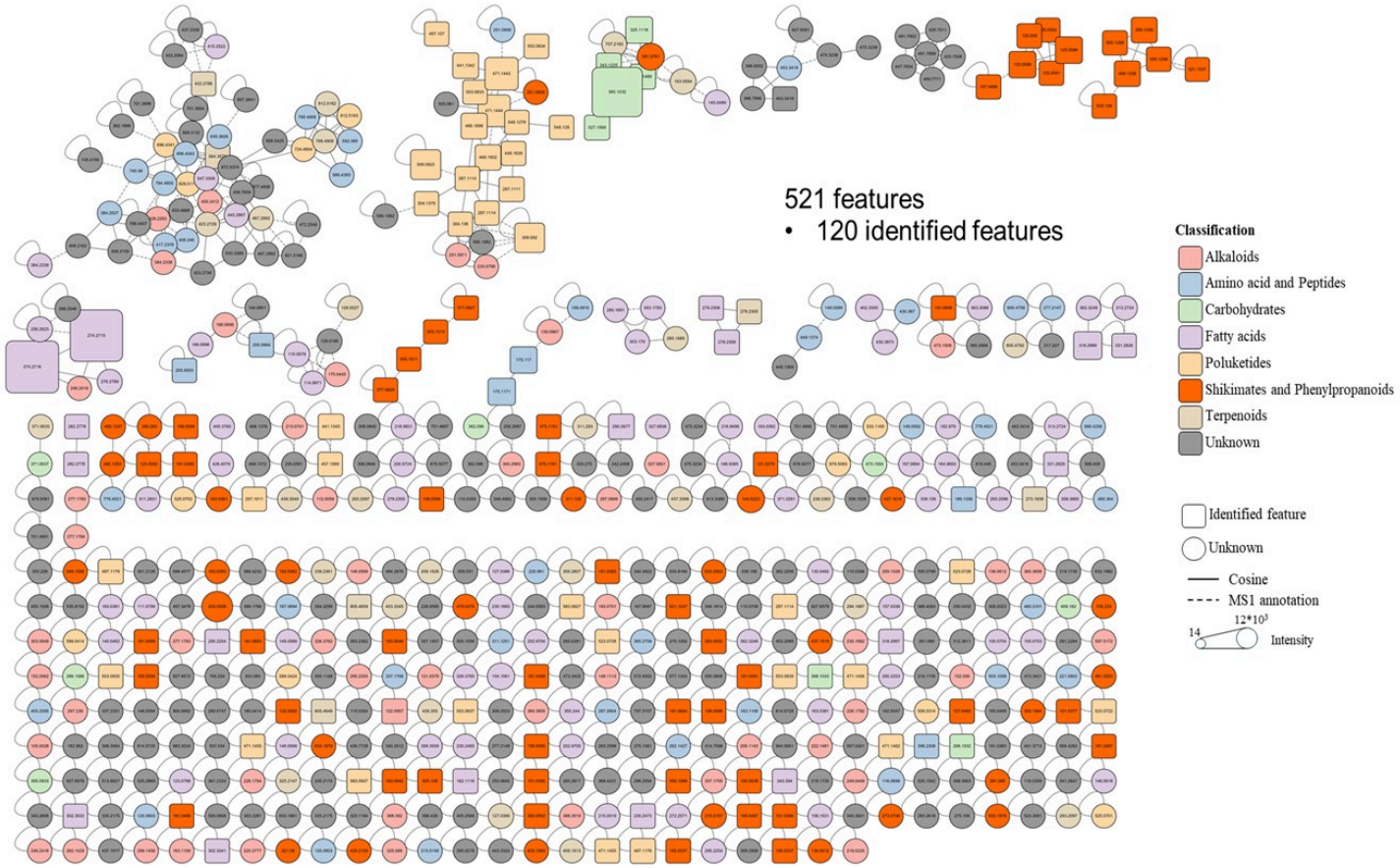

Figure 5

GNPS-based molecular networking of metabolites from the ethanol extract of *Curculigo orchioides*

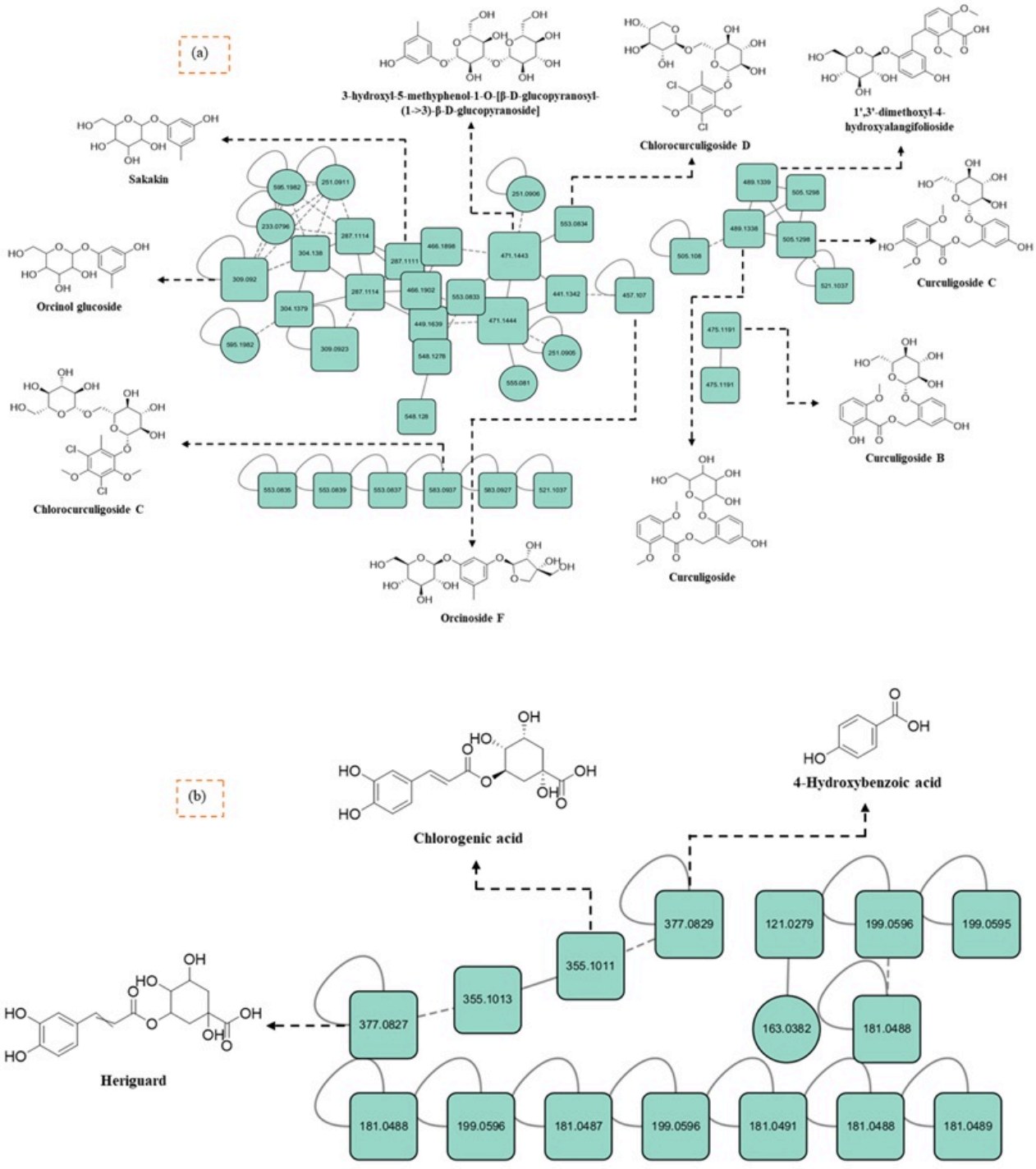

Figure 6

Molecular networking analysis of metabolites from the ethanol extract of *Curculigo orchioides*: (a) Enlarged view of Cluster I containing curculigoside-type phenolic glycosides and related derivatives; (b) Enlarged view of Cluster II corresponding to simple phenolic compounds and phenolic glycosides